

First Principle Calculations of Transition Metal Oxide, AgAlO₂, as Active Photocatalyst: Sustainable Alternative Sources of Energy

A. H. Reshak^{1,2,*}

¹Institute of Complex systems, FFPW, CENAKVA, University of South Bohemia in CB, Nove Hradý 37333, Czech Republic

²Center of Excellence Geopolymer and Green Technology, School of Material Engineering, University Malaysia Perlis, 01007 Kangar, Perlis, Malaysia

*E-mail: maalidph@yahoo.co.uk

Received: 4 May 2013 / Accepted: 30 May 2013 / Published: 1 July 2013

Electronic structure, optical properties and electronic charge density of transition metal oxide, AgAlO₂ as active photocatalyst are calculated using full potential linearize augmented plane wave (FP-LAPW) method within LDA, GGA, EVGGA and mBJ. The band gap is found to be indirect. Band gap value obtained with mBJ (2.69 eV) show better agreement with the experimental ones (2.81 eV) than the previous theoretical values (1.16 eV). Bond lengths and angles of Ag–O and Al–O are calculated, and good agreement is found with the experimental values than the previous calculations. Bonds exhibit greater percentage of covalent nature than the ionic nature. The optical properties are calculated and analyzed. The calculated absorption coefficient agree well with the experiment that the compound have maximum absorption in the UV region and the tail of the absorption is extend till 413.0 nm.

Keywords: photocatalyst, AgAlO₂; UV irradiation; DFT; mBJ

1. INTRODUCTION

Advancement in searching of sustainable and cheap alternative sources of energy has increased, particularly in solar energy field. Enhancement in solar energy conversion requires design of new materials. Solar energy conversion devices such as photovoltaic, photo-electrochemical cells and photocatalysts require cheap and efficient materials [1]. Photon absorption to produces electronically excited states, electron-hole pair separations and mobility of charges to produce either current or fuel are the common physical operations necessary for the primary stages of energy conversion by the devices [2]. Properties of materials such as band gap, electron-hole pair lifetime and electron and hole

mobility greatly affect the efficiency of solar energy conversion devices [3, 4]. Moreover, redox reactions on the surface of materials take place only if the energy of conduction band minimum lies above and for valence band maximum lies below the redox reaction free energies. Accurate information about the band edge position is the criteria that a material must fulfill to be active photoelectrode or photocatalyst [5].

Photocatalysis via oxide semiconductors has brought up attention of many people due to its high efficiency and wide applications in environmental pollution decomposition [6-8]. Extensive research has been carried out to investigate the photocatalytic properties of oxide semiconductors under visible light irradiation. Such as AgAlO_2 [9] ($E_g \sim 2.8$ eV) decomposes dye alizarin red (AR) photocatalytically and the decomposition rate increases up to 70 % under light irradiation.

Dissociation of water into hydrogen and oxygen using solar energy and metallic oxide semiconductor to produce hydrogen as clean energy has been a mission of mankind for many years. The important point to achieve this goal is to device a photocatalysts which is active and at the same time stable under visible light radiations [10]. The first photocatalyst, TiO_2 was discovered by Fujishima et al.'s four decades ago [11]. Since then a lot of efforts have been put to develop novel semiconductor photocatalysts that are able to decompose water with high efficiency. The excitation of the electrons in these photocatalysts takes place from O-2p orbitals to transition metals d orbitals with band gap exceeding 3.0 eV [12]. The band gap of most of the semiconductors photocatalyst developed till now are wider that are active only under Ultraviolet (UV) irradiation. The UV light occupies only 4% of the solar energy spectrum while visible light accounts for 43% of the whole solar energy spectrum. Many new materials with narrow band gap are studied which are active photocatalysts under visible light irradiation. Anion doping of transition metal oxides such as $\text{TiO}_{2-x}\text{N}_x$ [11], TaON could decrease the band gap [13-16]. Nitrides like Ta_3N_5 [13-15] are also visible light photocatalyst but most of them are unstable under irradiation. The hybridization of primal orbitals in multi metals oxides due to the orbitals of transition elements results in narrowing the band gap. As Zou et al., found that InNbO_4 and InTaO_4 split water into H and O_2 under visible light irradiation [17-20]. The electronic structures of multi metals oxides such as AgInW_2O_8 , [21] AgTaO_3 , [12] and AgNbO_3 , [22] show that their valence bands (VB) are formed by the hybridization of Ag-4d and O-2p states. While the conduction bands (CB) are formed by the hybridization of Ag-5s and other orbitals. Like In-5s state and W-5d state in AgW_2O_8 . In the previous study the individual contribution of Ag to valence and conduction band has not been shown clearly. We have calculated the electronic structure which shows the individual contribution of Ag to the conduction and valence band. The AgAlO_2 exists in two forms, hexagonal structure and orthorhombic structure. The later structure has dense polyhedron layers, which is considered to be more suitable for transferring electron-hole pairs [23]. Due to the structural advantage, orthorhombic crystal structure with space group $\text{Pna}2_1$ is used for the DFT calculations. AgAlO_2 was synthesized and characterized by Li j and Sleight A.W. [24] and Ouyang et al. [23]. In addition to the X-ray diffraction data Ouyang et al. performed a DFT calculation using CASTEP code. The DFT results obtained by Ouyang et al., disagree with the experimental data in the matter of the energy band gap. Since the energy bad gap is very important for the photocatalyst materials. Thus we have addressed ourselves to perform more accurate DFT calculation using the full potential (FP-LAPW) method with the modified Becke-Johnson potential (mBJ). The mBJ, allows the calculation of

band gaps with accuracy similar to the very expensive GW calculations [25]. It is a local approximation to an atomic “exact-exchange” potential and a screening term. The FP-LAPW method has proven to be one of the most accurate methods for the computation of the electronic structure of solids within DFT [26, 27].

2. COMPUTATIONAL DETAILS

Full potential linearized augmented plane wave (FP-LAPW) method is applied to calculate the electronic structure and optical properties of transition metal oxide, AgAlO_2 . FP-LAPW is based on density functional theory (DFT) as implemented in the WIEN2K code [28]. The DFT calculations are carried on minimized structure of AgAlO_2 . We have relaxed the geometry by minimizing the forces acting on each atom. We assume that the structure is totally relaxed when the forces on each atom reach values less than 1 mRy/a.u. The self-consistent field tolerance is 10^{-4} Ry. The electronic exchange-correlation energy is treated by generalized gradient approximation (GGA) and Engle Vosko generalized gradient approximation (EVGGA) which is more superior to local density approximation (LDA). We have used modified Becke-Johnson potential (mBJ) to obtain better band gap value that is mostly underestimated by LDA and GGA. The structure of transition metal oxide AgAlO_2 is orthorhombic with space group $\text{Pna}2_1$ (33). All the atoms in AgAlO_2 occupy Wyckoff position 4a. Crystal structure of AgAlO_2 consists of two types of tetrahedral, AgO_4 and AlO_4 [23]. The atomic positions and lattice constants are listed in the table-1 [23].

Table 1. Lattice constants and atomic positions in AgAlO_2 crystal [23].

Lattice parameters	Exp.			Calcd.			
	A (Å)	5.4306			5.2728		
	B (Å)	6.9802			5.7628		
	C (Å)	5.3751			5.3626		
Atomic coordinates	Atom	x	y	z	x	y	z
	Ag	0.0532	0.6268	0.9969	0.0598	0.6427	1.0069
	Al	0.0610	0.1251	0.0000	0.0706	0.1239	-0.0013
	O1	0.0311	0.0723	0.3209	0.0342	0.0679	0.3119
	O2	0.1283	0.6765	0.4345	0.1117	0.6681	0.4346

3. RESULTS AND DISCUSSION

3.1. Band structure and density of states

We have calculated the band structure using LDA, GGA, EVGGA and mBJ (Fig. 2) from these results we found that there is much difference in the band gap value of mBJ and the other three approximations that is LDA, GGA and EVGGA. This is due to the fact that mBJ is considered to be the best for calculating the energy gap. Our calculated band gap values for the LDA, GGA, EVGGA

and mBJ are 0.932 eV, 1.038 eV, 1.839 eV and 2.697 eV respectively. By examining Fig. 2 from (a) to (d) we can see that the conduction band minimum (CBM) is situated at the middle of the Brillouin zone, Γ point. While the valence band maximum is located between point U and R. From these observations we conclude that the band gap of the AgAlO_2 crystal is indirect. The band gap value using mBJ (2.70 eV) is better than other theoretical values 1.16 eV [23] and closer to experimental value 2.81 eV [23].

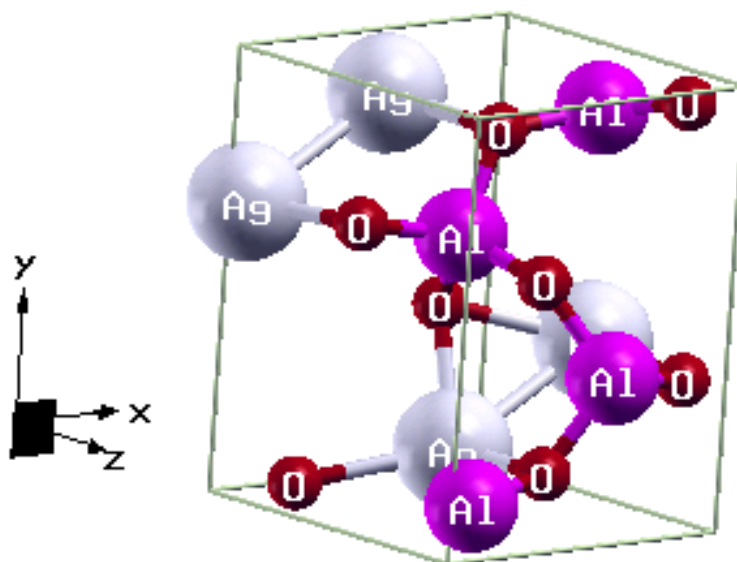
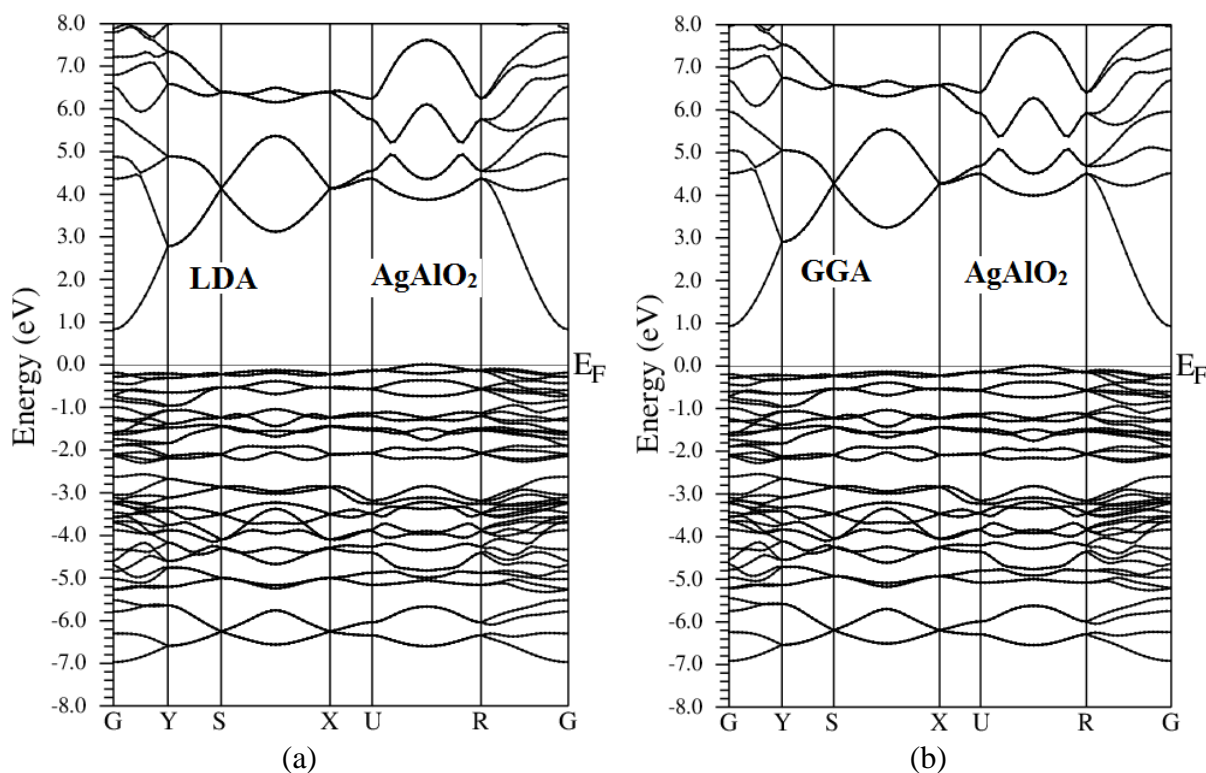


Figure 1. Unit cell structure of AgAlO_2 .



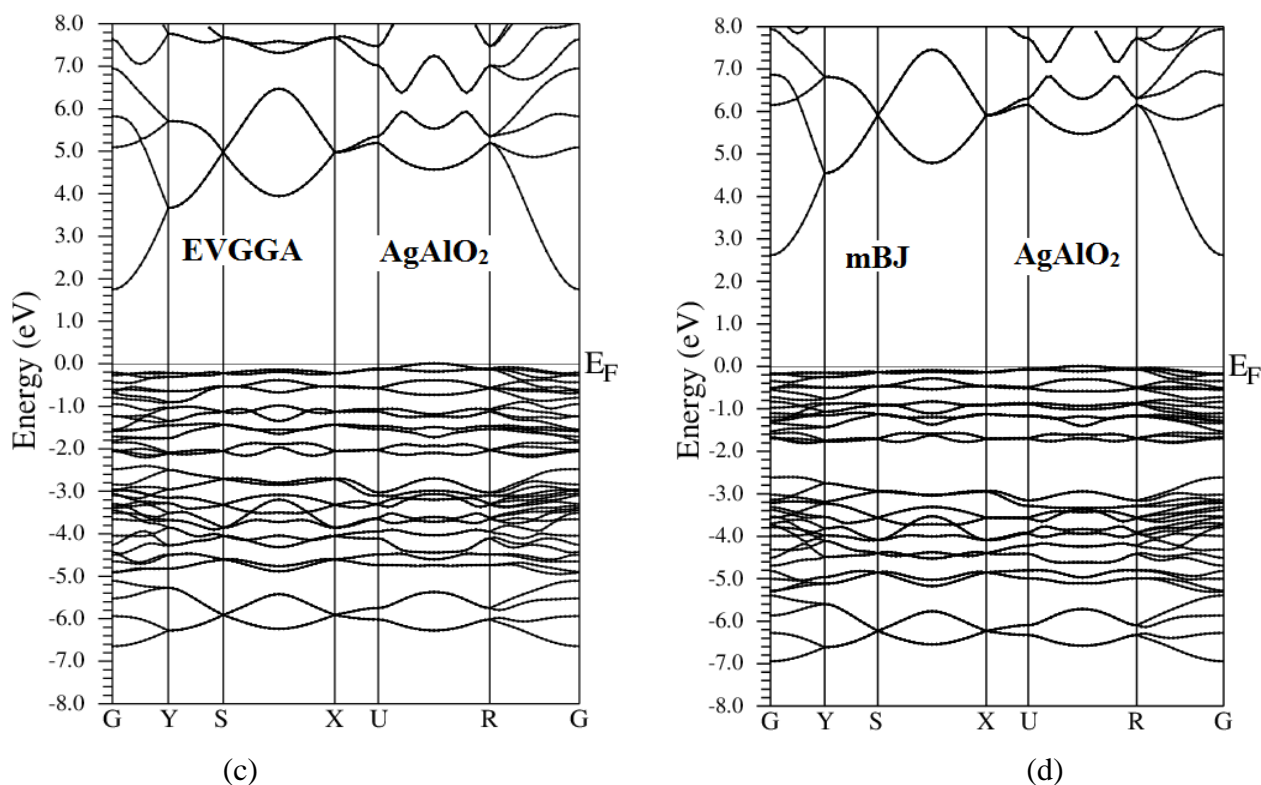
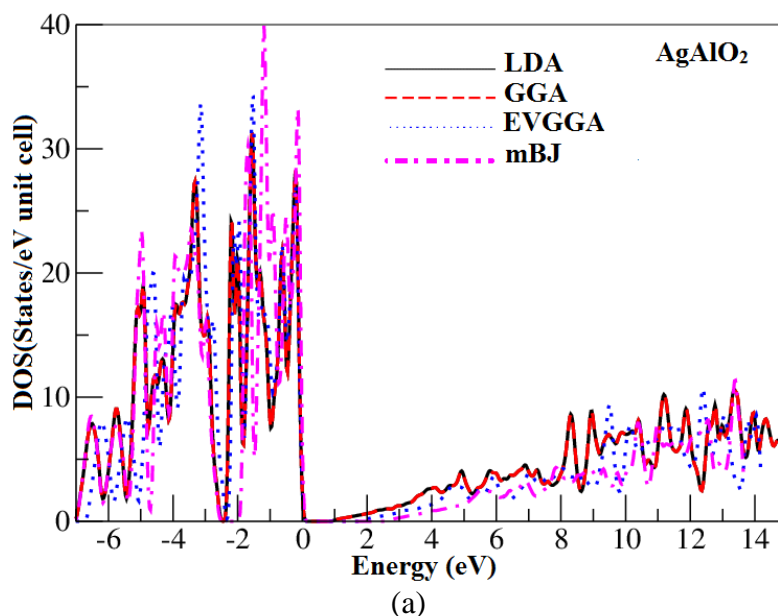
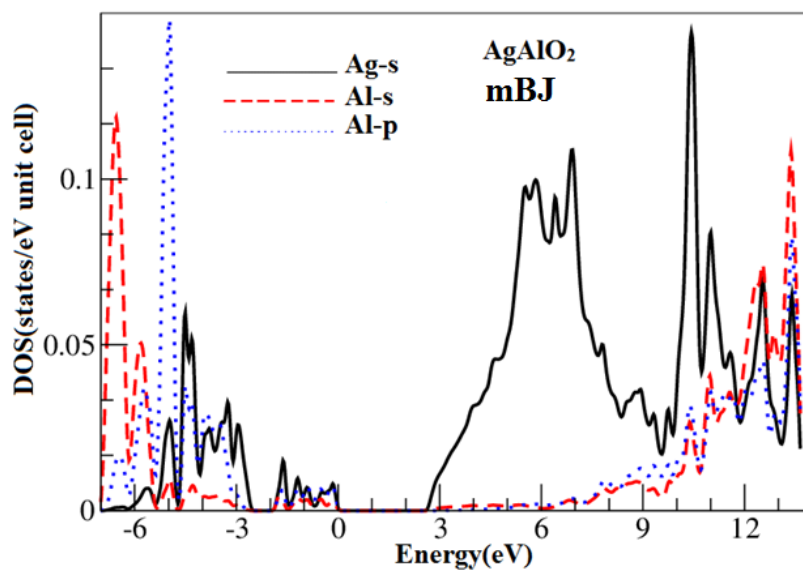


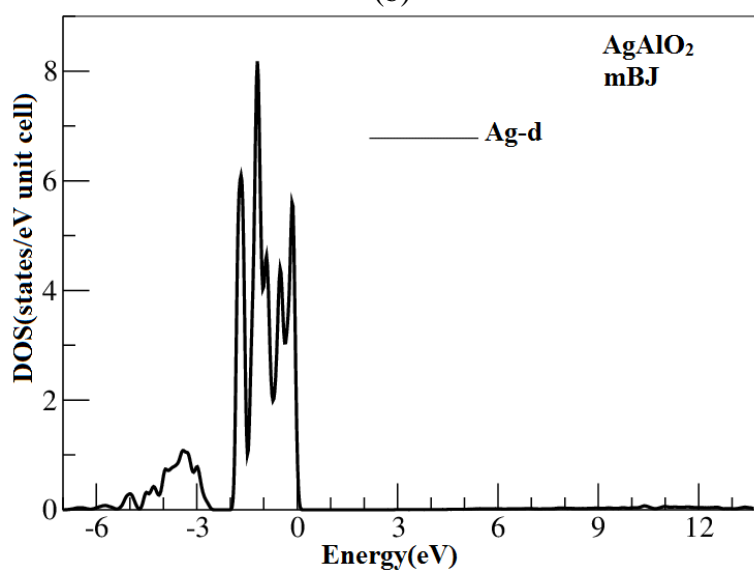
Figure 2. Calculated band structure of AgAlO_2 compound.

Hybridization and contributions of atomic states to the bands in electronic band structure can explicitly be view from the total density of states (TDOS) and partial density of states (PDOS). The TDOS (Fig. 3a) is calculated using LDA, GGA, EVGGA and mBJ. For the calculation of PDOS (Fig. 3 b, c, d) we used mBJ. It is clear from the PDOS that the main contribution to the valence band maximum comes from the Ag-d state alone and a minute participation from the hybridization of O_{1-p} and O_{2-p} orbitals.

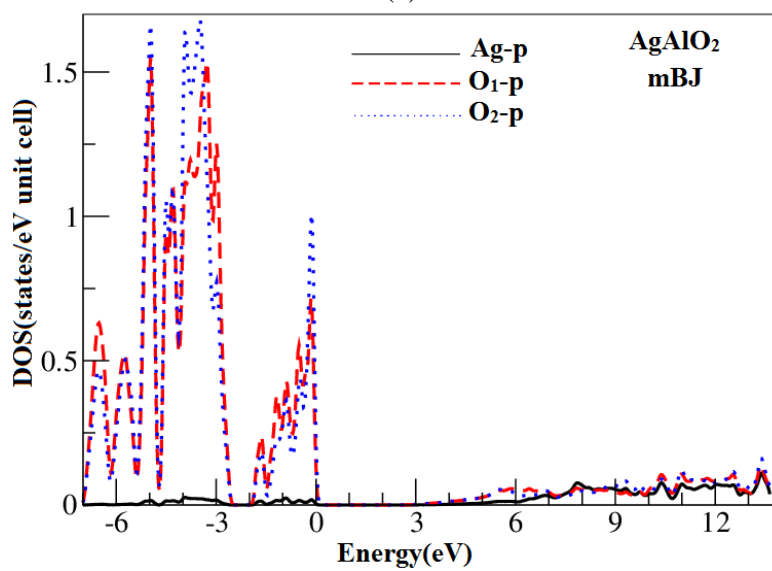




(b)



(c)



(d)

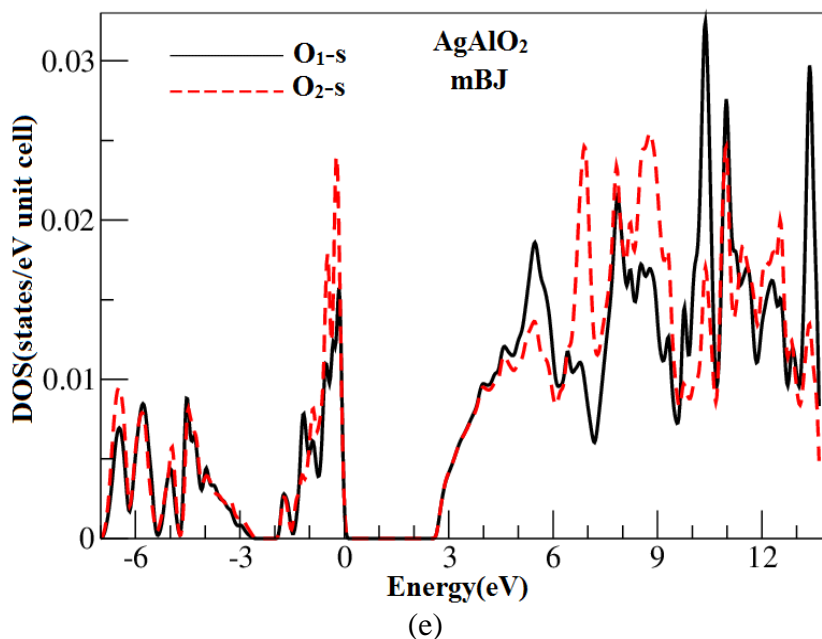


Figure 3. Calculated (a) Total density of states (States/eV unit cell) (b) PDOS of AgAlO_2 .

The valence band between energy range -3.0 eV and 5.0 eV is mainly due to the overlapping of O_{1-p} and O_{2-p} orbitals and a small contribution from the Ag-s state and Al-p state. The lowest part of the valence band is due to the hybridization of O_{1-p} and O_{2-p} orbitals.

The bottom of conduction band is mainly constructed of Ag-s and Ag-p orbitals while small contribution from Al and O is observed. Nature of chemical bonding can also be deduced from the hybridization of orbitals. Strong hybridization of states ensures covalent bonding whereas weak hybridization means strong ionic bond. There is a weak hybridization found between Al-p and Al-s around energy 4.0 eV and 6.0 eV. We can also see some overlapping states in the energy range -2.0 eV and -7.0 eV. Apart from these energy regions there is no strong hybridization which proves the existence of ionic bond mostly.

3.2. Electronic charge density

The electronic charge density is very much useful to identify the nature of chemical bonding. Using the mBJ xc potential we have calculated electronic charge density in (1 0 0) and (-1 1 0) crystallographic planes (Fig. 4 a, b). The electronegativity values for Ag, Al and O are 1.93, 1.61 and 3.44 respectively. Our calculated charge density shows dominant ionic character of chemical bonding as can be seen from the spherical lines around oxygen atom. The electronegativity difference is one major tool to determine the nature of bonding. Oxygen and silver has electronegativity difference of 1.51 indicates, thus the ionicity between O-Ag is about 32.15% , therefore the covalency is 67.85%. Whereas the difference in electronegativity between oxygen and Al is 1.83 that led to increase the ionicity between O-Al to be 41.01% and reduce the covalency to 58.99% with respect to O-Ag. Due to high electronegativity of oxygen most the valence charge is transferred from Ag and Al towards oxygen site. Hence, according to thermo scale the blue color indicates maximum charge concentration

site. Bond lengths and bond angles of AgAlO_2 are calculated. We would like to mention that in the $(-1\ 1\ 0)$ crystallographic plane only O and Al atoms are contribute while in the $(1\ 0\ 0)$ crystallographic plane the three atoms are contribute.

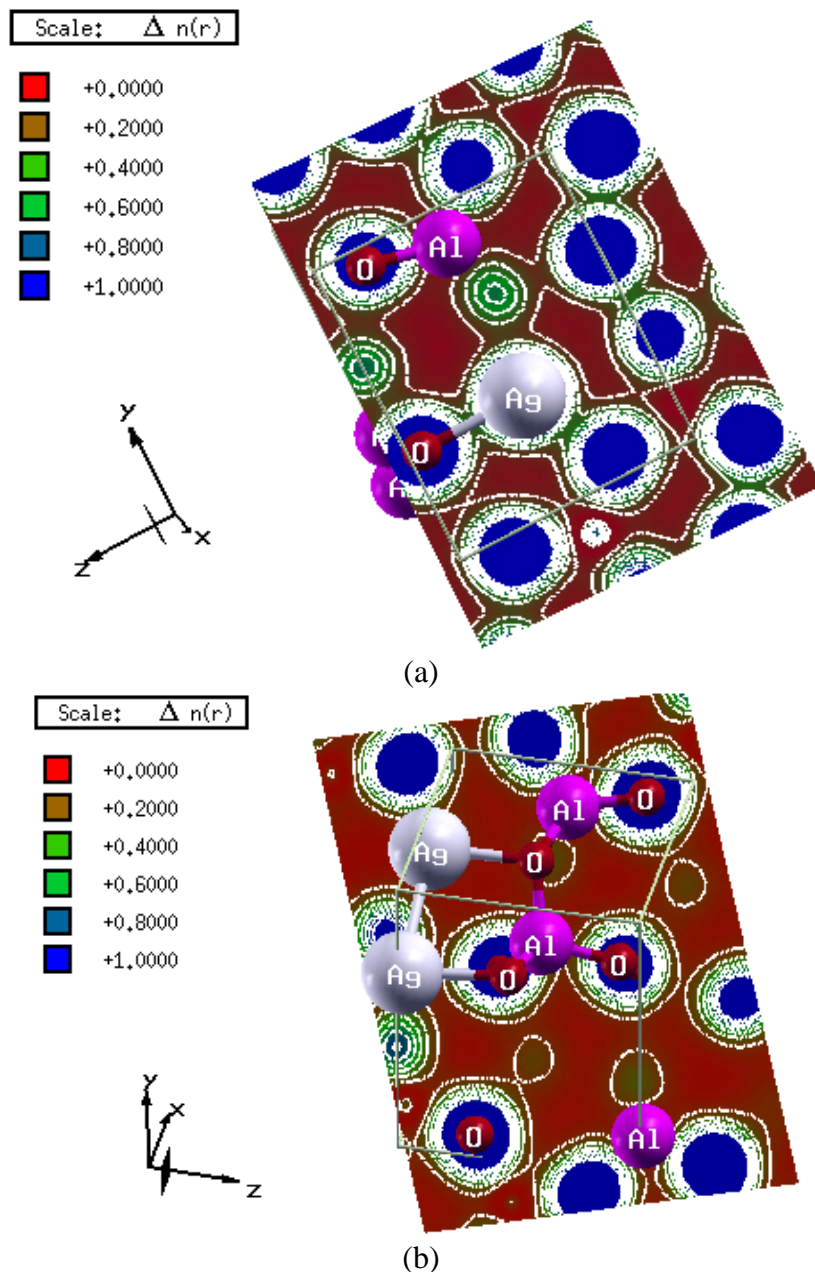


Figure 4. Electronic charge density of AgAlO_2 .

From the charge density of both planes we conclude that a considerable anisotropy is exist between $(1\ 0\ 0)$ and $(-1\ 1\ 0)$ crystallographic planes. Bond length of Ag–O in Ag_2O is smaller than 2.17\AA [23] and the bond length of Ag–O in AgTaO_3 , which has high photocatalytic activity in UV, is 2.46\AA [23]. Our calculated values of bond length of Ag–O lie in this range which matches the condition. Bond lengths and bond angles values of AgAlO_2 are listed in table 2.

Table 2. Calculated bond lengths and angles in AgAlO₂ crystal structure.

	Type	Values	
		Other work [23]	This work
Bond length (Å)	Al–O	1.754,1.760,1.761,1.771	1.748,1.738,1.737,1.750
	Ag–O	2.348, 2.360, 2.412, 2.477	2.287, 2.264, 2.315, 2.445
Bond angles (°)	O1–Ag–O2	100.9,103.9,107.3,131.6	110.40,92.89,128.79
	O1–Ag–O1	99.3	100.59
	O2–Ag–O2	109.8	104.24
	O1–Al–O2	107.7,108.9,109.0,110.0	109.62,109.05,107.90,108.60
	O1–Al–O1	110.2	110.30
	O2–Al–O2	111.1	111.37
	Ag–O1–Ag	83.5	78.60
	Ag–O2–Ag	86.5	94.85
	Al–O1–Al	136.4	140.21
	Al–O2–Al	132.9	127.21
	Ag–O1–Al	99.9,103.0,104.9,115.2	106.13,104.93,102.32,107.27
	Ag–O2–Al	100.9,102.1,109.1,115.7	101.21,121.33,106.31,100.07

3.3. Optical properties

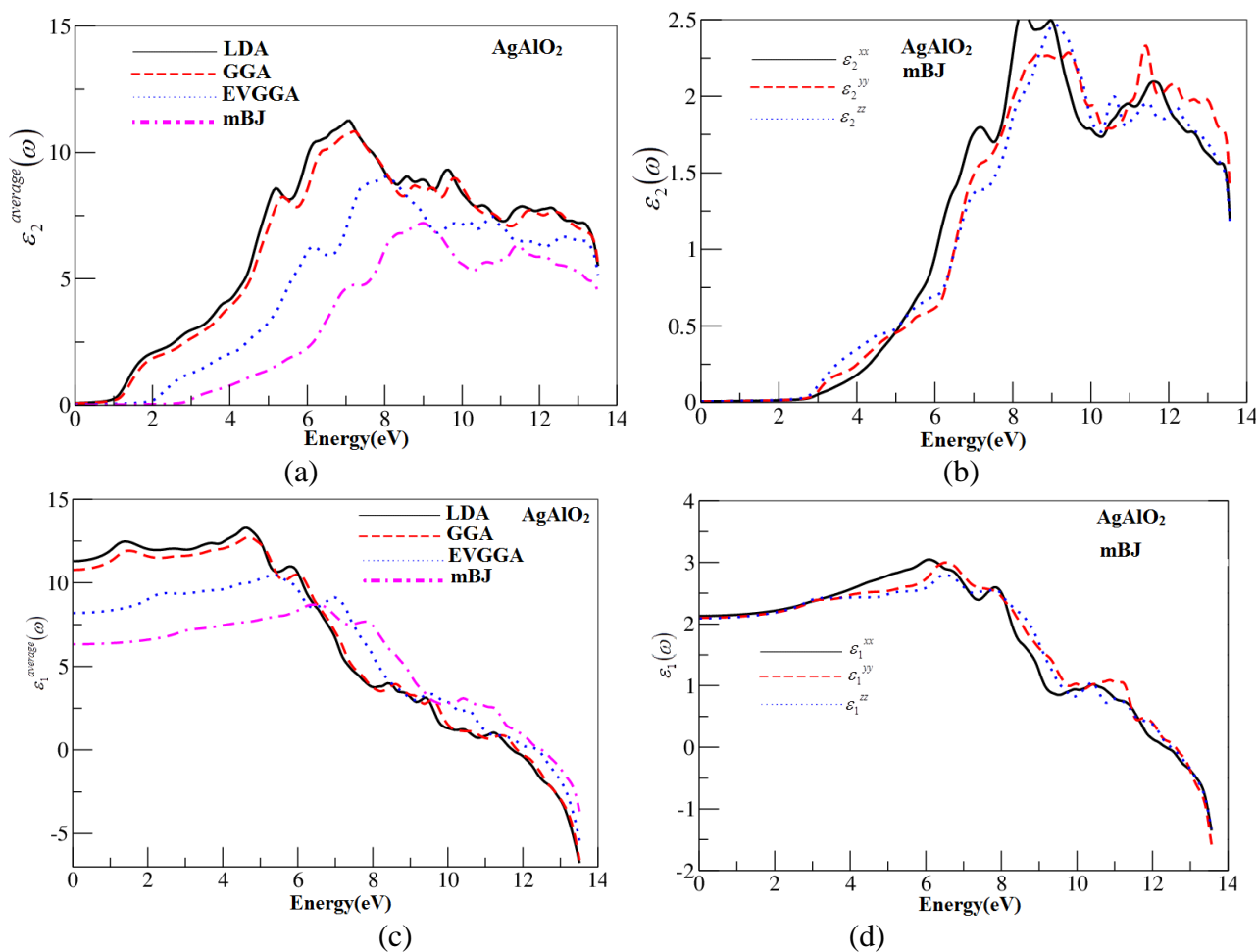


Figure 5. Calculated $\epsilon_2^{average}(\omega)$, $\epsilon_2(\omega)$, $\epsilon_1^{average}(\omega)$ and $\epsilon_1(\omega)$ for AgAlO₂.

Optical properties explore further knowledge about the electronic structure of the materials. We have calculated optical properties like dielectric function using LDA, GGA, EVGGA and mBJ. Real and imaginary part of dielectric function is calculated using mBJ. The crystal structure of AgAlO_2 is orthorhombic so the nonzero tensor components are three as follow $\varepsilon^{xx}(\omega)$, $\varepsilon^{yy}(\omega)$ and $\varepsilon^{zz}(\omega)$. In order to present the influence of using four types of XC on the optical properties we have calculated the average of the imaginary part, $\varepsilon_2^{average}(\omega)$ as shown in Fig. 5a, from which we can extract that the structure shift towards the higher energies as we move from LDA till mBJ. We should emphasis that mBJ give better energy gap close to the experimental ones. Thus we plot the $\varepsilon_2^{xx}(\omega)$, $\varepsilon_2^{yy}(\omega)$ and $\varepsilon_2^{zz}(\omega)$ obtained using mBJ as it is illustrated in Fig. 5b. We can see that in the lower energy between 5.0 eV and 9.0 eV the $\varepsilon^{xx}(\omega)$ component is the dominant one and the major peak occur at around 8.0 eV. The three components of dielectric function show anisotropy among each other throughout the structure.

The real part $\varepsilon_1^{xx}(\omega)$, $\varepsilon_1^{yy}(\omega)$, $\varepsilon_1^{zz}(\omega)$ and $\varepsilon_1^{average}(\omega)$ of the corresponding principal complex tensor components are obtained from the imaginary part of these principal complex tensor components by means of Kramers-Kronig transformation [29] as shown in Fig. 5 c and d . The values of $\varepsilon_1^{xx}(0)$, $\varepsilon_1^{yy}(0)$, $\varepsilon_1^{zz}(0)$ and $\varepsilon_1^{average}(0)$ were calculated and presented in Table 3. We note that a smaller energy gap yields a larger $\varepsilon_1(0)$ value. This could be explained on the basis of the Penn model [30]. Penn proposed a relation between $\varepsilon(0)$ and E_g , $\varepsilon(0) \approx 1 + (\hbar\omega_p/E_g)^2$. E_g is some kind of averaged energy gap which could be related to the real energy gap. It is clear that $\varepsilon(0)$ is inversely proportional with E_g . Hence a smaller E_g yields a larger $\varepsilon(0)$. Knowing the imaginary and real parts of the frequency dependent dielectric function we can obtain the reflectivity spectrum and the absorption coefficients.

Table 3. calculated $\varepsilon_1^{average}(0)$, $\varepsilon_1^{xx}(0)$, $\varepsilon_1^{yy}(0)$ and $\varepsilon_1^{zz}(0)$.

components	LDA	GGA	EVGGA	mBJ
$\varepsilon_1^{average}(0)$	11.320	10.870	8.220	6.350
$\varepsilon_1^{xx}(0)$	3.770	3.620	2.732	2.150
$\varepsilon_1^{yy}(0)$	3.670	3.540	2.733	2.120
$\varepsilon_1^{zz}(0)$	3.780	3.630	2.734	2.100

The calculated reflectivity spectrum as a function of wavelength is displayed in Fig. 6a. It is clear that the compound show the maximum reflectivity (50.0 %) at 90.0 nm (i.e in vacuum UV) and the tail of the reflectivity is (5.0 %) at 400.0 nm. In the visible range the compound process stable reflectivity of about 5.0 % . The absorption coefficient as function of the wavelength is plotted along with the experimental ones [23] (Fig. 6b). This figure exhibit that both of the experimental and theoretical curves are agree well that the compound have maximum absorption in the UV region and the tail of the absorption is extend till 413.0 nm. It is clear that from Fig. 6 a and b that AgAlO_2

possess 50.0 % reflection and around 33.0 % absorption in the UV region. We should emphasize that our finding is in good agreement with previous research work [23].

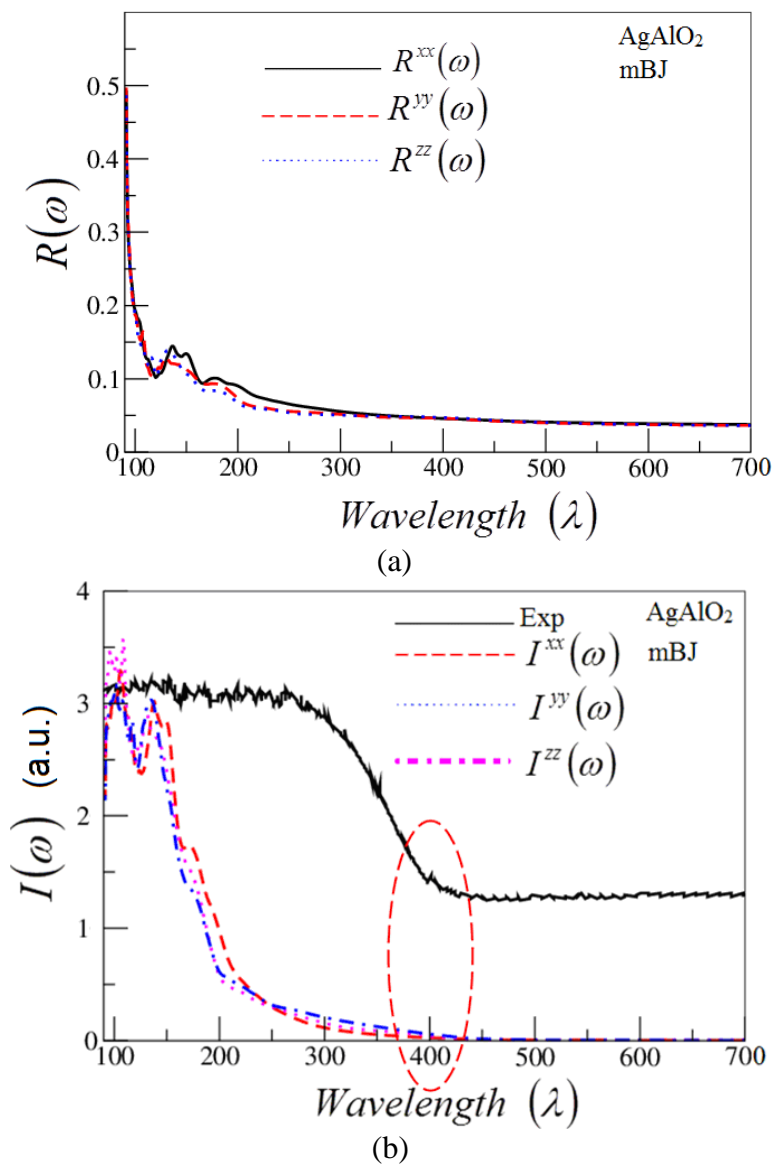


Figure 6. Reflectivity and absorption coefficient. (a) $R(\omega)$, (b) $I(\omega)$.

4. CONCLUSION

We have studied the electronic and optical properties of transition metal oxide, AgAlO₂. Full potential linearize augmented plane wave (FP-LAPW) method is used to calculate the band structure, TDOS, PDOS and optical properties. We have relaxed the geometry by minimizing the forces acting on each atom. We assume that the structure is totally relaxed when the forces on each atom reach values less than 1 mRy/a.u. We have performed band structure calculation and obtained better values relative to experimental results. Our mBJ result for the band gap (2.69 eV) is closed to experimental

value (2.81 eV) than the previous theoretical ones (1.61 eV). Which strongly support the fact that mBJ is accurate in finding the energy band gap of materials. From the PDOS we conclude that the valence band maximum is formed mostly from the Ag-d state. Optimization of the structure bring the bond lengths of Al–O and Ag–O close to the experimental values. Electronic charge density is calculated in the (1 0 0) and (-1 1 0) crystallographic planes and we found that the bonds exhibit greater percentage of covalent nature than the ionic nature. The optical properties are calculated and analyzed. The calculated absorption coefficient agrees well with the experiment that the compound have maximum absorption in the UV region and the tail of the absorption is extend till 413.0 nm.

ACKNOWLEDGEMENTS

This work was supported from the institutional research concept of the project CENAKVA (No. CZ.1.05/2.1.00/01.0024). School of Material Engineering, Malaysia University of Perlis, Malaysia.

References:

1. B. Coelho, A. C. Oliveira and A. Mendes, *Energy Environ. Sci.* 3 (2010) 1398.
2. M. X. Tan, P. E. Laibinis, S. T. Nguyen, J. M. Kesselman, C. E. Staton and N. S. Lewis, Principles and Applications of Semiconductor Photoelectrochemistry, ed. K. D. Karlin, Progress in Inorganic Chemistry, John Wiley & Sons, Inc., 1994, vol. 41.
3. W. Shockley, H. J. Queisser, *J. Appl. Phys.*, 32 (1961) 510.
4. T. Bak, J. Nowotny, M. Rekas and C. C. Sorrell, *Int. J. Hydrogen Energy*, 27 (2002) 991.
5. Maytal Caspary Toroker, Dalal K. Kanan, Nima Alidoust, Leah Y. Isseroff, Peilin Liao and Emily A. Carter, *Phys. Chem. Chem. Phys.*, 13 (2011)16644.
6. M. N. Iliev, M. V. Abrashev, V. N. Popov, V. G. Hadjiev, *Phys. Rev. B* 67 (2003) 212301.
7. Y. Okimoto, Y. Ogimoto, M. Matsubara, Y. Tomioka, T. Kageyama, T. Hasegawa, H. Koinuma, M. Kawasaki, and Y. Tokura, *Appl. Phys. Lett.* 80 (2002) 1031.
8. Y. Shen, T. Nakayama, M. Arai, O. Yanagisawa, M. Izumi. *J. Phys. Chem. Solids*, 63 (2002) 947.
9. S. X. Ouyang, H. T. Zhang, D. F. Li, T. Yu, J. H. Ye and Z. G. Zou, *J. Phys. Chem. B* 110 (2006) 11677.
10. Jinhua Ye, Zhigang Zou, Mitsutake Oshikiri, Akiyuki Matsushita, Masahiko Shimoda, Motoharu Imai, Toetsu Shishido, *Chemical Physics Letters* 356 (2002) 221.
11. K. Honda, A. Fujishima, *Nature* 238 (1972) 37.
12. R. Asahi, T. Morikawa and T. Ohwaki, et al. *Science*. 293 (2001) 269.
13. K. Domen, M. Hara, J. N. Kondo and T. Tanaka. *Bull. Chem. Soc. Jpn.* 73 (2000) 1307.
14. M. Hara, E. Chiba and A. Ishikawa, et al. *J. Phys. Chem. B*. 107 (2003) 13441.
15. M. Hara, G. Hitoki and T. Takata, et al. *Catal. Today*. 78 (2003) 555.
16. M. Hara, T. Takata, J. N. Kondo and K. Domen. *Catal. Today*. 90 (2004) 313.
17. Z. Zou, J. Ye and H. Arakawa. *Chem. Phys. Lett.* 332 (2000) 271.
18. Z. Zou, J. Ye, K. Sayama and H. Arakawa. *Nature* (London). 414 (2001) 625.
19. J. Ye, Z. Zou and H. Arakawa. et al. *J. Photochem. Photobiol. A: Chem.* 148 (2002) 79.
20. Z. Zou, Arakawa and H. *J. Photochem. Photobiol. A: Chem.* 158 (2003) 145.
21. J. Tang, Z. Zou and J. Ye. *J. Phys. Chem. B*. 107 (2003) 14265.
22. H.Kato, H. Kobayashi and A. Kudo, *A. J. Phys. Chem. B*. 106 (2002) 12441.
23. Shuxin Ouyang, Haitao Zhang, Dunfang Li, Tao Yu, Jinhua Ye, and Zhigang Zou, *J. Phys. Chem. B*. 110 (2006) 11677.
24. J. Li and A.W. Sleight, *Journal of Solid State Chemistry* 177 (2004) 889.
25. Fabien Tran and Peter Blaha *Phys. Rev. Lett.*102 (2009) 226401.
26. Shiwu Gao. *Computer Physics Communications*, 153 (2003) 190.

27. Karlheinz Schwarz. *Journal of Solid State Chemistry* 176 (2003) 319.
28. P. Blaha, K. Schwarz, G.K.H. Madsen, D. Kvanicka and J. Luitz. WIEN2K, An Augmented plane wave ρ Local Orbital Program for Calculating Crystal Properties Karlheinz Schwarz; Techn. Universitat Wien, Austria. ISBN: 3-9501031-1-1-2 (2001)
29. H. Tributsch and Z. Naturforsch. A 32A (1977) 972.
30. D.R. Penn. *Phys. Rev. B* 128 (1962) 2093.

© 2013 by ESG (www.electrochemsci.org)